Supporting information:

Electronic structure of the metal-organic interface of isolated ligand coated gold nanoparticles

Robin Schürmann,[a]* Evgenii Titov,[a] Kenny Ebel,[a] Sergio Kogikoski Jr.,[a] Amr Mostafa,[a] Peter Saalfrank,[a] Aleksandar R. Milosavljević,[b] Ilko Bald [a]*

[a] University of Potsdam, Institute of Chemistry, 14476 Potsdam, Germany

[b] Synchrotron SOLEIL, 91192 GIF-sur-YVETTE CEDEX, France

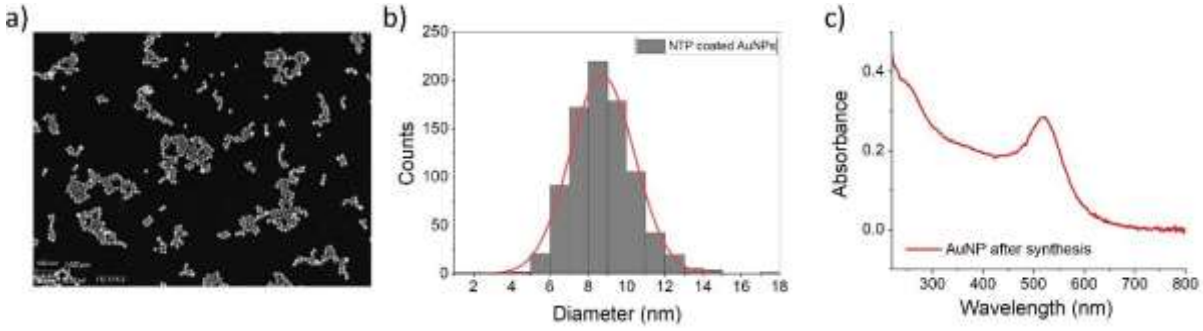

Figure S1: a) SEM image of NTP capped AuNPs on a Si substrate recorded with a Scanning Electron Microscope ZEISS Ultra plus. b) Size distribution of the NTP capped AuNPs determined with ImageJ 1.53e. c) UV-Vis spectrum of the AuNPs after synthesis recorded with a Nanodrop 2000 spectrophotometer (Thermo Scientific).

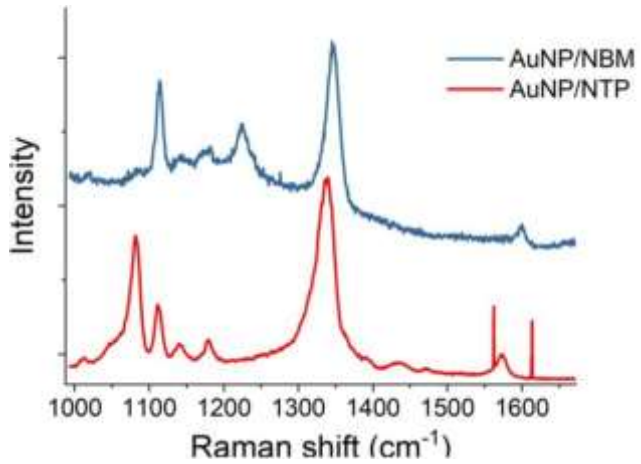

Figure S2: Raman spectra of NTP (red) and NBM (blue) coated AuNPs dried on a Si chip recorded with a Witec Alpha 300 confocal Raman microscope with a 785 nm laser (15 mW) focused with a Nikon 10x Objective (NA = 0.25).

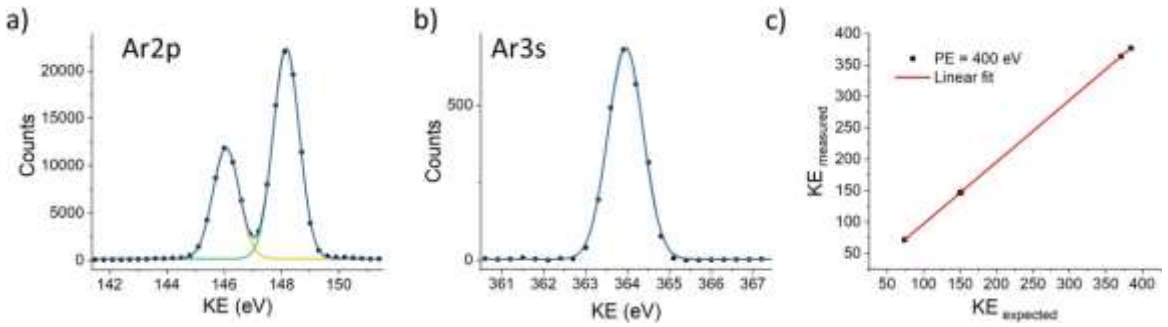

Figure S3: a) Ar2p spectrum recorded at PE= 400 eV. b) Ar3s spectrum recorded at PE= 400 eV. c) Calibration curve for the KE of the photoelectrons based on the 3p, 3s, 2p and 2s signals of the Ar carrier gas.

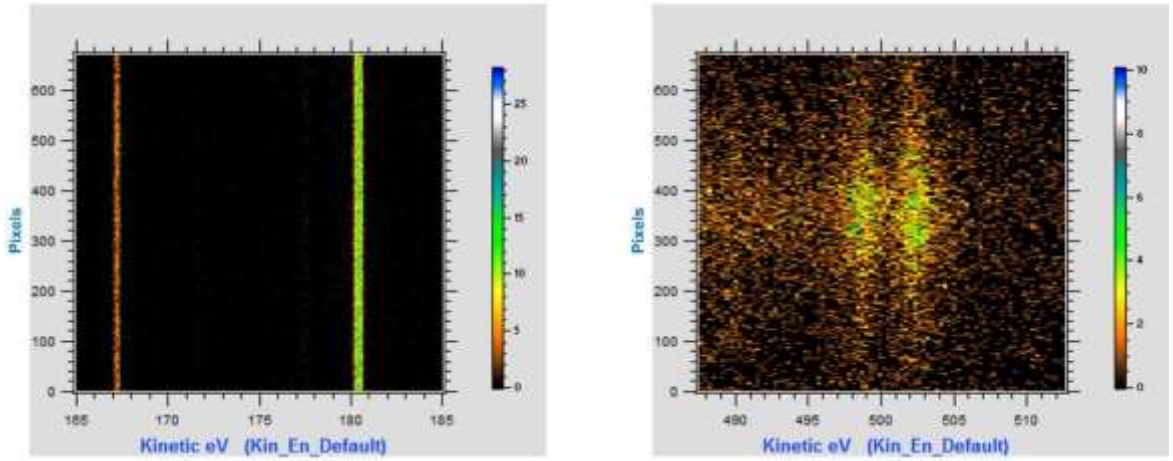

Figure S4: spectra of NTP capped AuNP beam, showing the Ar3s and Ar3p states of the carrier gas recorded at PE = 200 eV (left) and the Au4f states recorded at PE = 600 eV (right). The gas-phase signal and the signal in the center of the detector originating from the focused AuNP-beam can be easily distinguished by the unfocussed gas-molecules. An influence on the KE of the photoelectrons from Ar in the vicinity of the AuNP beam cannot be observed.

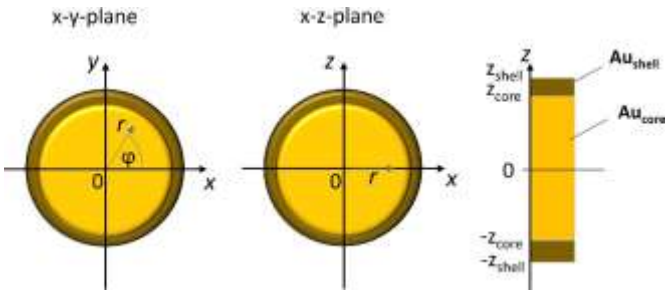

Figure S5: Scheme of an Au-Au core shell NP showing cross-sections along the x-y plane, x-z plane and a slice along the z-axis. The coordinates used in the calculation are presented in the scheme.

The XPS signal I_{AuNP} of a AuNP with radius r_{AuNP} is determined by calculating the signal I_z of a 1-dimensional slice along the z-axis of the AuNP (shown in Figure 3) and integrating over all slices in cylindrical coordinates r, φ, z (shown in Figure S5). Due to the symmetry of the AuNP I_z is independent of φ and I_{AuNP} can be written as:

$$I_{AuNP} = \int_0^{r_{AuNP}} \int_0^{2\pi} r \cdot I_z(r)\, dr\, d\varphi = 2\pi \cdot \int_0^{r_{AuNP}} r \cdot I_z(r)\, dr \qquad \text{(S1)}$$

Using formula (3) the intensity $I_z(r)$ of a 1-dimensional slice at a radial position *r* of an AuNP is given by:

$$I_{z,AuNP}(r) = I_0 \cdot \left(1 - e^{-\frac{2 \cdot z_{shell}(r)}{\lambda}}\right) \qquad \text{(S2)}$$

where $I_0$is the intensity of an infinitely thick Au-substrate and $z_{shell}(r) = \sqrt{r_{AuNP}{}^2 - r^2}$. In order to differentiate between the contributions of the signal originating from the core I_{core} and from the shell I_{shell}, their $I_z(r)$ are calculated separately. Using equation (3) $I_{z,core}$ can be written as:

$$I_{z,core} = I_0 \cdot \left(e^{-\frac{z_{shell}(r) - z_{core}(r)}{\lambda}} - e^{-\frac{z_{shell}(r) + z_{core}(r)}{\lambda}}\right) \qquad \text{(S3)}$$

By combining equation S1 and S3 I_{core} is given by:

$$I_{core} = 2 \cdot \pi \cdot I_0 \int_0^{r_{AuNP}} r \cdot \left(e^{-\frac{z_{shell}(r) - z_{core}(r)}{\lambda}} - e^{-\frac{z_{shell}(r) + z_{core}(r)}{\lambda}}\right) dr \qquad \text{(S4)}$$

Consequently, with $I_{AuNP} = I_{core} + I_{shell}$ and equation (S4) an expression for I_{shell} is obtained.

$$I_{shell} = 2 \cdot \pi \cdot I_0 \int_0^{r_{AuNP}} r \cdot \left(1 - e^{-\frac{z_{shell}(r) - z_{core}(r)}{\lambda}} + e^{-\frac{z_{shell}(r) + z_{core}(r)}{\lambda}} - e^{-\frac{2 z_{shell}(r)}{\lambda}}\right) dr \qquad \text{(S5)}$$

Since only the relative intensities of I_{core} and I_{shell} are relevant for the interpretation of the experimental XPS-data, the intensities in the equations (4) and (5) are normalized by I_0.

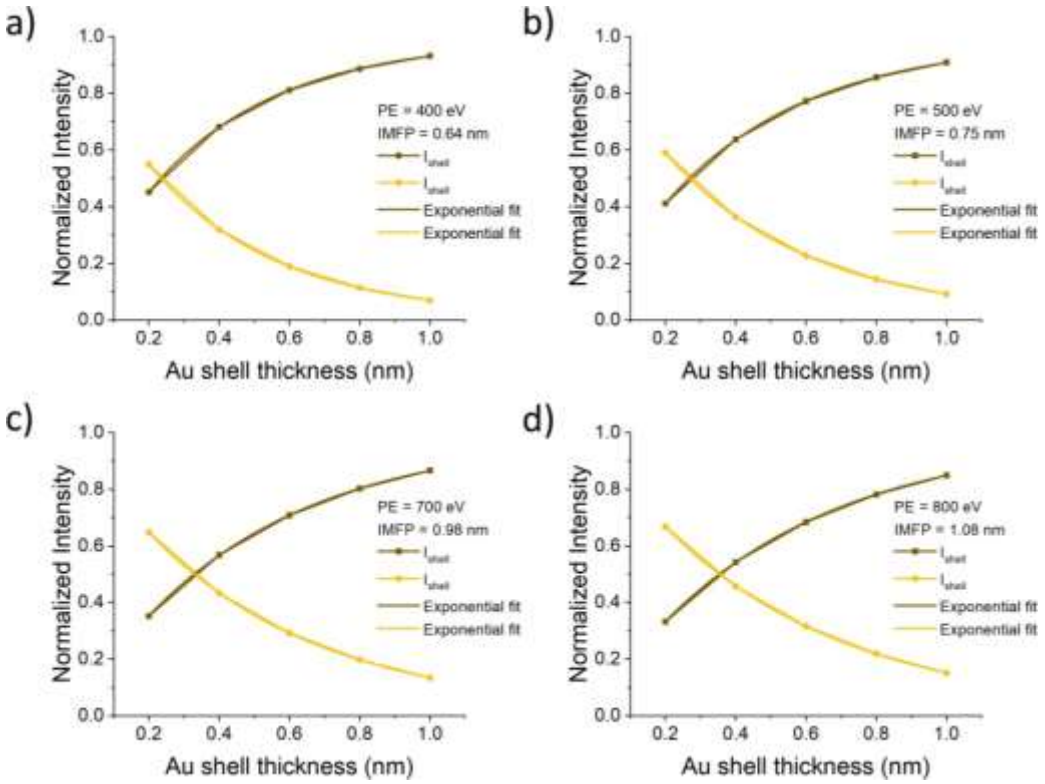

Figure S6: Calculated XPS signal intensities for Au_{shell} and Au_{core} of 10 nm AuNPs for different Au shell thickness and inelastic mean free paths (IMFP) of the photoelectrons, namely 0.64 nm (a), 0.75 nm (b), 0.98 nm (c), 1.08 nm (d).

Table S1: Au 4f orbital shifts ``gold − complex'' in eV calculated at the B3LYP/TZVP+ANO-R level of theory. Note that the orbital energies are negative and, hence, positive shifts correspond to downward orbital shifts. All considered systems are neutral.

	Au_1	Au_2	Au_{10}
NTP	1.279	0.928	0.357
NBM	0.972	0.714	0.321

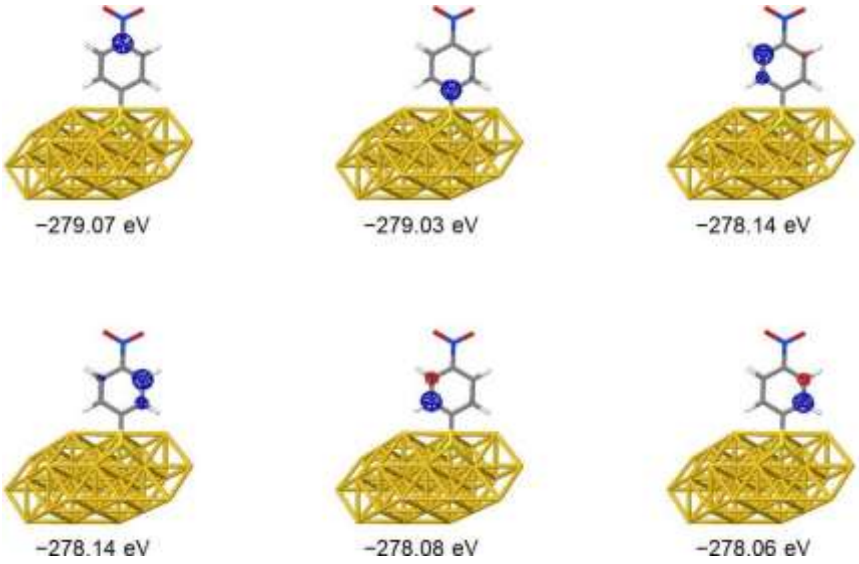

Figure S7: C 1s orbitals and orbital energies for the Au_{30}–NTP complex calculated at the B3LYP/TZVP+LANL2TZ(f) level of theory.

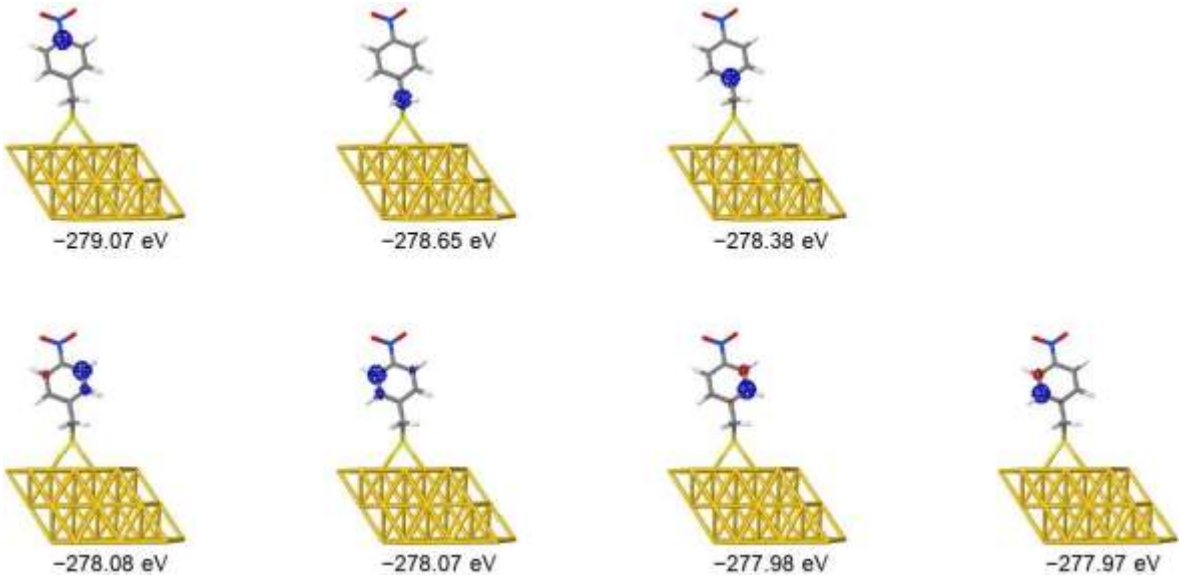

Figure S8: C 1s orbitals and orbital energies for the Au_{30}–NBM complex calculated at the B3LYP/TZVP+LANL2TZ(f) level of theory.